

1 **Rapid embryonic cell cycles defer the establishment of heterochromatin by Eggless/SetDB1 in *Drosophila*.**

2 **Running title:** Cell cycle slowing times heterochromatin formation

3 Charles A. Seller, Chun-Yi Cho, and Patrick H. O'Farrell¹

4 University of California, San Francisco, Dept. of Biochemistry and Biophysics, San Francisco, CA, USA

5 1. Corresponding author: Phone 415 476-4707, Email: ofarrell@cgl.ucsf.edu

6

7

8 **Rapid embryonic cell cycles defer the establishment of heterochromatin by Eggless/SetDB1 in *Drosophila*.**

9 **Running title:** Cell cycle slowing times heterochromatin formation

10 Charles A. Seller, Chun-Yi Cho, and Patrick H. O'Farrell

11 **Acquisition of chromatin modifications during embryogenesis distinguishes different regions of an initially**
12 **naïve genome. In many organisms, repetitive DNA is packaged into constitutive heterochromatin that is**
13 **marked by di/tri methylation of histone H3K9 and the associated protein HP1a. These modifications enforce**
14 **the unique epigenetic properties of heterochromatin. However, in the early *Drosophila melanogaster* embryo**
15 **the heterochromatin lacks these modifications which only appear later when rapid embryonic cell cycles slow**
16 **down at the Mid-Blastula Transition or MBT. Here we focus on the initial steps restoring heterochromatic**
17 **modifications in the embryo. We describe the JabbaTrap, a technique for inactivating maternally provided**
18 **proteins in embryos. Using the JabbaTrap we reveal a major requirement for the methyltransferase**
19 **Eggless/SetDB1 in the establishment of heterochromatin. In contrast, other methyltransferases contribute**
20 **minimally. Live-imaging reveals that endogenous Eggless gradually accumulates on chromatin in interphase,**
21 **but then dissociates in mitosis and its accumulation must restart in the next cell cycle. Cell cycle slowing as the**
22 **embryo approaches the MBT permits increasing accumulation and action of Eggless at its targets.**

23 **Experimental manipulation of interphase duration shows that cell cycle speed regulates Eggless. We propose**
24 **that developmental slowing of the cell cycle times embryonic heterochromatin formation.**

25 The transformation of the egg into a multicellular organism remains one of the wonders of the natural
26 world. By the 18th century, scientists viewed this process as an example of epigenesis, where the simple and
27 formless fertilized egg progressively differentiates into a complex organized creature. We now know that the
28 transformation of the egg from simple to differentiated is preceded and caused by a similar transformation of
29 the naïve zygotic genome. The division of the genome into distinct euchromatin and heterochromatin is the
30 most obvious example of genomic differentiation. Eukaryotes constitutively package significant portions of their
31 genomes into heterochromatin (Brown 1966), and such packaging is critical for the stability of the genome

32 (Janssen et al. 2018). Constitutive heterochromatin displays conserved genetic and molecular properties that are
33 stably transmitted throughout development and across generations (Allshire and Madhani 2018). However,
34 embryogenesis interrupts this stability, and the early embryos of many animals lack true heterochromatin. Thus,
35 embryogenesis involves the restoration of heterochromatin, and this restoration can serve as a paradigm for
36 how epigenetic control of the genome arises during development.

37 In general, constitutive heterochromatin is transcriptionally silent, late replicating, and low in
38 recombination. The chromosomes of many species contain large megabase sized arrays of simple repeated
39 sequences, known as satellite DNA, surrounding their centromeres, and it is this pericentric repetitive DNA that
40 composes the bulk of the constitutive heterochromatin. Although heterochromatin was originally defined
41 cytologically – it remains condensed throughout the cell cycle – modern studies often emphasize the set of
42 conserved modifications to its chromatin. Heterochromatic nucleosomes are hypoacetylated and di/tri-
43 methylated at lysine 9 on the N-terminal tail of Histone H3 (hereafter H3K9me2/3). The deposition of
44 H3K9me2/3 creates a binding site for HP1 proteins (Eissenberg and Elgin 2014) and HP1 can oligomerize and
45 recruit additional heterochromatin factors which could then generate a distinct compartment in the nucleus.

46 Studies in *Drosophila* have historically made major contributions to our understanding of
47 heterochromatin (Elgin and Reuter 2013). Many key regulators of heterochromatin were discovered in genetic
48 screens for modifiers of Position Effect Variegation (PEV), a phenomenon where a reporter gene close to the
49 border between euchromatin and heterochromatin is differentially silenced among different cells in an all or
50 none fashion. Currently over 150 distinct genetic loci are reported to impact PEV, highlighting the complexity of
51 heterochromatin control. Critically, the pathway depositing H3K9me2/3-HP1a forms the regulatory core and null
52 mutations in *Su(var)2-5* (HP1a), and replacement of H3K9 with arginine (H3K9R) to block its modification are
53 both lethal (Eissenberg et al. 1990; Penke et al. 2016, 2018). The *Drosophila* genome encodes three K9
54 methyltransferases: *Su(var)3-9*, *eggless/SetDB1*, and *G9a*, and all three have been reported to modify PEV (Mis
55 et al. 2006; Brower-Toland et al. 2009). To our knowledge, no study has systematically assessed the
56 contributions of these enzymes to the establishment of heterochromatin in the embryo.

57 Although a dispensable gene (Tschiersch et al. 1994), *Su(var)3-9* is the best studied and most strongly
58 associated with the constitutive heterochromatin in the literature (Elgin and Reuter 2013; Allshire and Madhani
59 2018). Loss of *Su(var)3-9* leads to strong suppression of PEV. Additionally, analysis of salivary gland polytene
60 chromosomes revealed that *Su(var)3-9* is required for the localization of H3K9me2/3 and HP1a to the
61 chromocenter, the region where the pericentric heterochromatin clusters in the nucleus (Schotta et al. 2002).
62 *G9a* is dispensable in *Drosophila* and thought to function primarily at euchromatic sites (Seum et al. 2007b).
63 Eggless is the only essential K9 methyltransferase. Studies in larval and adult stages have emphasized that *egg*
64 plays a specialized role in depositing H3K9me2/3 at Chromosome 4 (Seum et al. 2007a; Tzeng et al. 2007) which
65 forms a distinct chromatin structure (Riddle et al. 2012). H3K9me2/3-HP1a is missing from chromosome 4 in the
66 polytene chromosomes of *egg* mutants, but unaffected at the chromocenter. These findings suggested that *egg*
67 does not regulate the pericentric heterochromatin. Further analysis demonstrated that *egg* is also required in
68 both the soma and germline for the completion of oogenesis (Clough et al. 2007, 2014; Wang et al. 2011). Egg
69 plays a major role in the piRNA pathway that silences transposons in the germline (Rangan et al. 2011; Sienski et
70 al. 2015; Yu et al. 2015). Although they have yielded much information, these studies focused on the
71 maintenance of heterochromatin, but not on its embryonic emergence.

72 Like most animals, the *Drosophila* embryo begins development with a stereotyped series of rapid cell
73 cycles following fertilization that are driven by high levels of cyclin-CDK1 activity (Farrell and O'Farrell 2014;
74 Yuan et al. 2016). These divisions occur in a syncytium, are synchronous, lack gap phases, and run entirely by
75 maternal gene products. The first 8 divisions are remarkably fast (each with an interphase of less than 4 min)
76 and occur deep within the embryo. Starting at cycle 9, nuclei migrate to the surface of the embryo to form a
77 syncytial blastoderm. Interphase duration extends progressively and incrementally from cycle 10 through 13
78 (from 7 min to 14 min). Beginning at cycle 14 the embryo enters the Mid-Blastula Transition, or MBT, a
79 conserved embryonic transformation. At the MBT, the cell cycle slows down dramatically due to the
80 programmed downregulation of CDK1, and the embryo switches its focus from cell proliferation to
81 morphogenesis and patterning. Concomitantly, the zygotic genome activates in full and stable patterns of

82 histone modification emerge (Chen et al. 2013; Li et al. 2014). Zygotic transcription then drives morphogenetic
83 events like cellularization and gastrulation. The slowing of the cell cycle is critical for the developmental events
84 that follow it because short cell cycles inhibit productive transcription (Shermoen and O'Farrell 1991; Strong et
85 al. 2017). Additionally, rapid cell cycles could impair the installation of chromatin modifications that regulate
86 gene expression, but to our knowledge no direct examination of the enzymes installing these modifications at
87 the MBT exists.

88 Prior work from our lab has outlined a series of changes made to the heterochromatin as the embryo
89 reaches the MBT. Surprisingly, the conserved features of heterochromatin appear at different times during
90 embryogenesis, indicating that diverse mechanisms contribute to the introduction of its otherwise well
91 correlated properties. The compaction of satellite DNA is evident as early as cycle 8, before the onset of late
92 replication and the association of H3K9me2/3-HP1a (Shermoen et al. 2010). Upon Cdk1 downregulation at the
93 MBT select satellite repeats then recruit the protein Rif1 which acts to delay their replication (Seller and
94 O'Farrell 2018). During the prolonged interphase 14 some satellites become stably associated with H3K9me2/3-
95 HP1a (Yuan and O'Farrell 2016), and by the cycle 15 the satellites coalesce into a clear chromocenter. The
96 emergence of the key features of heterochromatin follows a stereotyped schedule centered around the MBT,
97 and we suggest that this period represents the establishment of mature heterochromatin in the embryo.
98 Following the MBT the satellites faithfully exhibit these characteristics for the rest of development. We want to
99 understand the developmental control of establishment, but first need to discover the key molecules in this
100 process. Here we identify the methyltransferase Egg as a key initiator and propose that heterochromatin
101 formation is timed by the limitations imposed on Egg by rapid embryonic cell cycles.

102 **RESULTS**

103 **The JabbaTrap inactivates maternally deposited proteins by rapid mislocalization**

104 The power of fly genetics is nearly incontestable, but the early embryo does present a significant
105 challenge to it. Over 80% of genes are supplied to the embryo as maternally deposited mRNA and protein, and

106 consequently development of the embryo up to the MBT does not require zygotic gene products. Removing
107 maternal contributions is of course possible when the mother fly is mutant for the gene under study, but many
108 interesting genes have essential zygotic functions. Germline clone techniques can serve as a workaround for the
109 study of essential genes, but only if the mutation under study does not interfere with oogenesis. Here the
110 genetics of *egg* serves as a clear example of the dilemma. Zygotic null mutants for *egg* have poor viability, and
111 *egg* is required at multiple points in both the soma and germline during oogenesis. Therefore, no study has
112 examined a potential role for *egg* during the establishment of the heterochromatin in the early embryo.

113 Alternative strategies for removing maternally supplied function are needed. Although some methods
114 do exist, they depend on the stability of their targets and can be slow and incomplete. Here we developed an
115 approach in the spirit of the Anchors Away technique (Haruki et al. 2008) for inactivating GFP tagged proteins in
116 the early embryo by selective mislocalization. As schematized in Fig 1A, target proteins are mislocalized by the
117 expression of an anti-GFP nanobody (Rothbauer et al. 2008) fused to the lipid droplet binding protein Jabba (Li
118 et al. 2012), which we call the JabbaTrap. Lipid droplets act as storage organelles during early embryogenesis
119 and are distributed throughout the cytoplasm (Welte 2015), and we reasoned that trapping nuclear proteins on
120 lipid droplets would block their function.

121 As an initial test, we targeted the protein Orc2, an essential component of the Origin Recognition
122 Complex (ORC). Orc2 has a highly reproducible pattern of localization during the cell cycle and is required for S
123 phase completion in mitotic cycles (Baldinger and Gossen 2009). Orc2-GFP embryos were injected with either
124 water (control) or synthesized JabbaTrap mRNA and then immediately filmed by confocal microscopy. In control
125 injected embryos Orc2-GFP resided in the nucleus in interphase, diffused into the cytoplasm upon mitotic entry,
126 and then rapidly bound along the anaphase chromosomes in preparation for the next S phase (Fig. 1B, first row).
127 In contrast, in embryos expressing the JabbaTrap, Orc2-GFP displayed aberrant localization. During the first
128 mitosis following injection, Orc2 was present on numerous cytoplasmic puncta as well as on membranous
129 structures surrounding the mitotic spindle (Fig. 1B, second row, 3:00, Supplemental Movie 1). Upon mitotic exit
130 Orc2 coalesced around the reforming nuclear envelope but did not bind to the chromosomes and remained in

131 the cytoplasm during the subsequent S phase. As expected, without chromatin bound Orc2 nuclei entered
132 mitosis after a delay but then underwent catastrophic anaphase bridging (Fig. 1B, second row, 19:00).
133 Importantly, expression of the JabbaTrap in embryos with untagged Orc2 did not disrupt cell cycle progression
134 (Fig. 1B, third row).

135 As a second test we used the same approach to mislocalize the protein Zelda, a pioneering transcription
136 factor required for proper zygotic genome activation (Liang et al. 2008). We injected *sfGFP-zelda; His2Av-RFP*
137 embryos with JabbaTrap mRNA during nuclear cycle 10, and then followed them by time lapse microscopy.
138 Zelda is a nuclear protein that forms foci on interphase chromatin. Expression of the JabbaTrap blocked the
139 nuclear localization of Zelda near the injection site (Fig. 1D). Embryos with JabbaTrapped Zelda failed
140 dramatically at cellularization and gastrulation, events known to require zygotic transcription. Nuclei near the
141 injection site did not undergo the shape changes characteristic of cellularization, but rather appeared swollen
142 and ultimately fell out of the cortical layer (Fig. 1C).

143 Next, we established transgenic lines for the JabbaTrap. Lipid droplets form during oogenesis and we
144 reasoned that by driving the expression of the JabbaTrap with a Maternal-tubulin Gal4, which activates
145 transcription after egg chamber budding, embryos would already have the JabbaTrap deployed when they begin
146 developing. To test this idea, we injected purified mCherry-HP1a and GFP-HP1a proteins into embryos collected
147 from mothers expressing the JabbaTrap. Following protein injection, we immediately filmed embryos by
148 confocal microscopy. As expected mCherry-HP1a quickly localized to the nucleus after its delivery (Fig. 1E, in
149 magenta). In contrast, injected GFP-HP1a localized to numerous cytoplasmic puncta and was excluded from the
150 nucleus throughout the cell cycle (Fig. 1E, in green).

151 As a further test we used our transgenic JabbaTrap to block the Polycomb group protein *Su(z)12*, an
152 essential component of PRC2 with well characterized mutant phenotypes at different stages of development.
153 Polycomb group proteins are required for the repression of the homeotic genes and determine their anterior
154 boundary of expression in the developing embryo. However, zygotic null mutants for *Su(z)12* die during L1 or L2

155 stages without any obvious polycomb phenotypes, likely due to the confounding impact of maternal supply
156 (Birve et al. 2001). Germline clone analysis using null alleles revealed that *Su(z)12* is also essential for oogenesis.
157 To test an embryonic function for *Su(z)12*, Birve et al. crossed females with germline clones of the weak *Su(z)12*²
158 allele with males heterozygous for a deficiency spanning the gene region. The resulting embryos misexpressed
159 the homeotic gene *Ubx*, a classic polycomb phenotype. To determine if our JabbaTrap approach could produce a
160 similar loss of function situation we tagged *Su(z)12* with sfGFP at its endogenous locus using CRISPR-Cas9
161 (Supplemental Fig. 1) and expressed our JabbaTrap maternally in this background. This resulted in high
162 embryonic lethality (2.7% hatch rate, n = 150) and clear misexpression of *Ubx* (Fig. 1F). In control embryos
163 *Su(z)12* formed nuclear foci in gastrulating embryos – a stage when polycomb bodies first become evident. In
164 contrast, expression of the JabbaTrap prevented nuclear localization of *Su(z)12* (Fig. 1G)

165 **Eggless is required for the establishment of the heterochromatin at the MBT**

166 Our prior study characterized the appearance of H3K9me2/3 during early embryogenesis using antibody
167 staining and observed little evidence of this modification before cycle 13 (Yuan and O'Farrell 2016). To
168 understand the dynamics of H3K9me2 deposition we took advantage of the Fab-based live endogenous
169 modification (FabLEM) technique (Hayashi-Takanaka et al. 2011). We injected GFP-HP1a expressing embryos
170 with Cy5 labeled Fab fragments recognizing H3K9me2 to follow both modifications in real time over cycles 12-14
171 (Fig. 2A, Supplemental Movie 2). In doing so we made several interesting observations. Within a cell cycle, the
172 K9me2 Fab accumulated progressively in chromatin foci as interphase proceeded, but the signal dissipated upon
173 entry into mitosis. At telophase the K9me2 Fab was again recruited to chromatin, and in each successive cycle
174 the intensity of this telophase signal increased. We interpret this as an indication of the amount of H3K9me2
175 carried over from the previous cell cycle, and by cycle 14 this telophase signal is significant (Fig. 2A, Cycle 14
176 0:00). Additionally, as interphase duration increased in successive cycles the chromatin bound Fab signal
177 accumulated to greater extent. This was particularly dramatic during interphase 14 when the K9me2 Fab signal
178 became quite bright and eventually covered the chromocenter (Fig. 2A, Cycle 14 64:00). The recruitment of
179 HP1a to chromatin foci closely paralleled the appearance of K9me2 Fab signal. We conclude that H3K9me2

180 increases progressively during cycles 12-14 as interphase duration extends, and that modifications deposited in
181 earlier cycles can carry over to later cycles.

182 Because the association of HP1a during interphase 14 tracked closely the accumulation of H3K9me2 we
183 used its recruitment to assess the contributions of the different *Drosophila* K9 methyltransferases to the
184 establishment of heterochromatin. As mentioned above, *G9a* and *Su(var)3-9* are dispensable genes, allowing us
185 to analyze embryos from null backgrounds. Embryos of either *WT*, *G9a^{RG5}*, or *Su(var)3-9^{06/17}* background were
186 injected with mCherry-HP1a and the recruitment of this protein to heterochromatin was recorded during cycle
187 14 by confocal microscopy. The timing and extent of HP1a recruitment to heterochromatic foci appeared similar
188 between *WT* and *G9a^{RG5}* embryos, and by the end of cycle 14 these foci had fused into a chromocenter (Fig. 2B,
189 2nd row). Surprisingly, although HP1a recruitment in *Su(var)3-9* embryos was altered, with both delayed and
190 reduced appearance of foci, these embryos still formed significant amounts of heterochromatin (Fig. 2B, 3rd
191 row). TALE-light probes allow us to follow specific satellite repeats in live embryos (Yuan et al. 2014). Using this
192 technique, we previously documented that the 359 bp repeat, a 20 Mb sized satellite on the X chromosome,
193 acquires H3K9me2/3-HP1a during cycle 14. By co-injecting mCherry-HP1a and 359-TALE-GFP proteins we
194 observed that neither *G9a* or *Su(var)3-9* was required for the recruitment of HP1a at 359 (Fig. 2C). We conclude
195 that *G9a* is not required for the establishment of heterochromatic modifications, and that *Su(var)3-9*, while
196 contributing, is not required for initiating HP1a recruitment.

197 Our development of the JabbaTrapping technique allowed us to assess the contributions of *eggless* to
198 establishment. First, we used CRISPR-Cas9 to tag endogenous Egg with GFP at its N-terminus (Supplemental Fig.
199 1), the resulting line was healthy and fertile indicating that our tag is functional. In JabbaTrap expressing
200 embryos GFP-Egg was mislocalized to small cytoplasmic puncta and blocked from entering the nucleus
201 throughout the cell cycle (Supplemental Fig. 2). Like the behavior of lipid droplets, these puncta were prominent
202 and surrounded the nuclei during the syncytial cycles but appeared to drop out of the cortical layer by cycle 14.
203 Additionally, embryos with JabbaTrapped Egg had poor viability (15% hatch rate, n = 283).

204 To assess the effect that mislocalization of Egg had on the establishment of the heterochromatin
205 JabbaTrap control and JabbaTrapped GFP-Egg embryos were injected with mCherry-HP1a and imaged by
206 confocal microscopy during cycle 14. In control embryos HP1a formed foci that grew in number and intensity
207 over time, and then ultimately fused into a large chromocenter. Once established during cycle 14, HP1a
208 association at the chromocenter is inherited in subsequent cell cycles, and nuclei begin interphase 15 with HP1a
209 enriched at the chromocenter (Fig. 2D, Supplemental Movie 3). In contrast, the mislocalization of Egg
210 substantially reduced and delayed the recruitment of HP1a to heterochromatic foci (Fig. 2D, Supplemental
211 Movie 4). Even by the end of cycle 14 the amount of HP1a marked heterochromatin was clearly less than
212 control, indicating that some of the sequences that normally acquire HP1a fail to do so in the absence of Egg.
213 Indeed, following JabbaTrapping of Egg, HP1a did not localize to the 359 bp repeat (Fig. 2G). In control embryos,
214 HP1a was recruited to the 359 bp repeat during the middle of interphase 14, but JabbaTrapping of Egg blocked
215 this accumulation (Fig. 2F and Supplemental Fig.3). Additionally, the deficit in HP1a localization to the
216 chromocenter was inherited into cycle 15 (Fig. 2D).

217 Next, we directly examined K9 methylation using the K9me2-Fab. JabbaTrapping Egg completely
218 prevented the appearance of H3K9me2 at 359 during cycle 14, and significantly reduced its accumulation
219 throughout the chromocenter (Fig. 2E). However, we note that the mislocalization of Egg did not completely
220 abolish the formation of either HP1a or H3K9me2-Fab foci, these could represent sequences that rely on
221 methylation by G9a or Su(var)3-9, or that recruit HP1a by a methylation independent pathway. To confirm these
222 results, we stained fixed gastrulation stage embryos for HP1a and H3K9me3. Control embryos had a clear
223 chromocenter that stained positively for both modifications. In contrast, in JabbaTrapped Egg embryos K9me3
224 was undetectable, and although a few HP1a foci were present, they were faint and disperse (Supplemental Fig.
225 3C).

226 We conclude that Egg plays a major role in the restoration of repressive chromatin modifications on the
227 satellite DNA during the MBT and is required for the establishment of H3K9me2/3-HP1a at the 359 bp repeat. In
228 addition, Egg is unique in this respect among the three K9 methyltransferases in *Drosophila*.

229 **Live imaging of Egg reveals the dynamics of heterochromatin establishment**

230 Although prior studies had documented enrichment of Egg at Chromosome 4 and not to the
231 chromocenter, our JabbaTrap experiments revealed a major role for Egg in the formation of the constitutive
232 heterochromatin. We thus decided to examine the localization dynamics of Egg by live confocal microscopy in
233 the early embryo. However, endogenous levels of Egg were relatively low in the embryo making long term and
234 high-resolution imaging of GFP-Egg difficult. To solve this issue, we took advantage of the HaloTag system in
235 combination with the JF549 fluorescent dye which has improved brightness and photostability compared to
236 EGFP (Grimm et al. 2015). We used CRISPR-Cas9 to insert the HaloTag at the N-terminus of the endogenous *egg*
237 gene. The resulting flies were viable and fertile. After permeabilization with Citrasolv, the HaloTag ligand JF549
238 could directly enter the embryo allowing easy *in vivo* labeling. Examination of embryos with both Halo549-Egg
239 and GFP-Egg revealed that the two proteins had equivalent localization during late cycle 14 (Supplemental Fig.
240 4D). Additionally, the JF549 labeling was specific to embryos containing the Halotag (Supplemental Fig. 4E).

241 In late cycle 14 embryos Halo-Egg colocalized with GFP-HP1a and the H3K9me2-Fab at the satellite
242 sequences (Fig. 3A). Interestingly, the Egg signal was contained within a broader nuclear region labeled with
243 HP1a and K9me2 indicating that at this stage, when the heterochromatin has matured, Egg does not fill the
244 entire heterochromatin domain. By altering the parental origin of tagged *eggless* we determined that the Egg
245 present during cycle 14 is primarily maternally supplied (Supplemental Fig. 4C). Not all satellite sequences
246 acquire H3K9me2/3 during the MBT, the 1.686 repeat remains free of this modification until much later in
247 development (Yuan and O'Farrell 2016). In accordance with this fact, by using different TALE-light probes we see
248 that Egg binds to 359, but not to 1.686 (Fig. 3B). Eggless contains a tandem tudor domain (Supplemental Fig. 4A),
249 a structure known to mediate chromatin targeting in other proteins. Therefore, we generated a transgene to
250 express a version of GFP-Egg lacking the tandem tudor sequence and expressed this mutant protein in the early
251 embryo. We observed that the tandem tudor domain was required for the nuclear localization of Egg
252 (Supplemental Fig. 4B). For comparison we also examined the localization of the G9a methyltransferase because

253 our previous experiments demonstrated that it was not required for heterochromatin establishment. Unlike Egg,
254 G9a did not co-localize with HP1a during cycle 14, but rather was diffusely present in the nucleus (Fig. 3C).

255 As early as cycle 10, we documented multiple bright foci of Halo-Egg in the nucleus (Fig. 3D). In contrast,
256 at this stage HP1a is uniformly distributed in the nucleus and not enriched to heterochromatic foci. Live imaging
257 of Halo549-Egg together with GFP-HP1a over the next 4 cell cycles yielded several interesting observations (Fig.
258 3D). During each interphase Egg accumulated progressively to bright chromatin foci after a short (2 min.) delay
259 following exit from the prior mitosis (Fig. 3D, Supplemental Movies 5 and 6). By tracking individual Egg foci over
260 multiple frames of our records we documented a pattern (Fig. 3D, circled foci, and Supplemental Movie 5)
261 where a small focus of Egg would appear and then be joined by a focus of HP1a within minutes. The two
262 proteins then grew in intensity over the course of interphase. Upon entry into mitosis, HP1a dissociated from
263 chromatin and Egg followed slightly later. Overall, the recruitment of Egg to specific foci preceded that of HP1a
264 within the cell cycle and during development. The longer interphase durations in later cell cycles correlated with
265 greater accumulation and longer retention of Egg at its chromatin targets. For instance, during the brief 7 min.
266 interphase 11 Egg foci grew in number and intensity for 5.5 min., but then these foci rapidly disappeared as the
267 nucleus prepared for mitosis (Fig. 3D). In contrast, during the prolonged interphase 14 Egg foci were brighter
268 and remained on chromatin for the duration of our records. In conclusion, the recruitment of Egg to its
269 chromatin substrates is a progressive process occurring in each cell cycle that begins early in embryogenesis (at
270 least by cycle 10). These observations together with our real time records of H3K9me2 accumulation (Fig. 2A)
271 indicate that changes in interphase duration may time the formation of the heterochromatin.

272 Our records also revealed some diversity in behaviors. The appearance and growth of Egg foci did not
273 follow a single schedule, apparently different sequences recruit the protein at different times during interphase.
274 By cycle 14, it was clear that HP1a was recruited to some foci before Egg, a possible indication of the
275 H3K9me2/3 carried over from prior cell cycles. Additionally, some foci of HP1a did not co-localize with Egg,
276 which is consistent with our observation that a small amount of HP1a was still recruited after JabbaTrapping Egg
277 (Fig. 2D).

278 **Windei, an activator of Eggless, localizes to the heterochromatin in the early embryo**

279 Studies on both Egg, and its mammalian counterpart SETDB1 suggest that it requires a cofactor for
280 efficient methylation of H3K9. SETDB1 alone has very poor methyltransferase activity (Schultz et al. 2002), but it
281 is greatly stimulated when in complex with the protein mAM/MCAF1 (Wang et al. 2003). The *Drosophila*
282 ortholog of mAM known as *windei* (*wde*) was suggested to play a similar role in flies (Koch et al. 2009). The
283 phenotypes of *wde* and *egg* mutants are similar, and *wde* is also required during oogenesis. The two proteins
284 physically interact and were reported to co-localize at Chromosome 4 in polytene preparations, but both were
285 absent from the chromocenter. Because we have documented a role for Egg at the constitutive heterochromatin
286 in the early embryo we decided to examine Wde during this stage.

287 Immunostaining revealed that Wde localizes to the heterochromatin during its establishment at the
288 MBT. Wde was enriched in the DAPI intense apical portion of the nucleus where the satellite sequences reside
289 (Fig. 4A). Additionally, we observed broad colocalization between Wde and HP1a late in cycle 14 (Fig. 4B).
290 Because we had shown that the association of H3K9me2/3-HP1a to the 359 bp repeat required Egg we wanted
291 to know if Wde also bound to this satellite. TALE-light staining revealed that Wde does localize to 359 (Fig. 4C).
292 By co-IP western blotting we documented that GFP-Egg interacts with endogenous Wde in the early embryo (Fig.
293 4D), in agreement with what was reported in S2 cells (Koch et al. 2009). We also noticed that Wde was found in
294 the cytoplasm in embryos with JabbaTrapped Egg (Fig. 4E), indicating that the JabbaTrap may be useful to
295 mislocalize entire protein complexes. We conclude that in the early embryo Wde co-localizes with Egg during
296 the formation of the constitutive heterochromatin.

297 **Interphase duration controls Egg recruitment to and establishment of the heterochromatin.**

298 To examine the relationship between heterochromatin establishment and the cell cycle more directly
299 we injected Halo-Egg embryos with Cy5 labeled histone proteins, to visualize the chromatin, and imaged at high
300 frame rate. As described previously, Egg accumulated to multiple nuclear foci during interphase with a slight
301 delay following exit from the previous mitosis (Supplemental Movie 6). These foci abruptly disappeared upon

302 chromosome condensation at prophase (Fig. 5A, Supplemental Movie 6). It appears that mitosis inhibits the
303 chromatin association of Egg, which would prevent it from methylating H3K9.

304 Our observations over cycles 11-14 (Fig. 3D) when the cell cycle slows naturally suggested that
305 interphase duration limits the recruitment of Eggless to the heterochromatin. To test this idea, we wanted to
306 experimentally arrest the cell cycle in interphase and examine the consequences on Egg localization. Embryos
307 injected with dsRNA against the 3 mitotic cyclins (A, B, and B3) during cycle 11 arrest during interphase 13
308 (McCleland and O'Farrell 2008). We then followed Halo549-Egg and GFP-HP1a by confocal microscopy during
309 this prolonged interphase. In control embryos, Egg accumulated at nuclear foci over interphase, but by 13 min.
310 into the cycle these foci began disappearing as chromosomes entered mitosis (Fig. 5B). In contrast, arresting
311 nuclei in interphase permitted continued accumulation and chromatin association of Egg for the duration of our
312 records (Fig. 5B, Supplemental Movie 7). Egg foci in arrested nuclei became brighter and larger than in the
313 control and resembled Egg foci observed late in cycle 14 (Fig. 3D). This effect was paralleled by increased
314 recruitment of HP1a to large heterochromatic foci (Supplemental Movie 7). We conclude that mitosis limits Egg
315 accumulation and persistence on chromatin.

316 Our model would predict that reducing interphase duration would decrease the amount of
317 heterochromatin established by Egg, so we shortened interphase using a *grapes* (*chk1*) mutant and counted the
318 number of GFP-HP1a foci per nucleus as a readout. Embryos mutant for *grp* have faster cell cycles because the
319 replication checkpoint is required for the progressive prolongation of interphase during cycles 11-13 (Sibon et al.
320 1997). Mutant *grp* embryos enter mitosis 13 before completing DNA replication and exhibit an 8 min. instead of
321 14 min. interphase. In heterozygous control embryos the number of HP1a foci increased over the initial 11-12
322 min. of interphase, reaching a maximum of over 14 foci per nucleus (Fig. 5 C and D), before declining rapidly as
323 nuclei prepare for mitosis. In contrast, in *grp* embryos HP1a began to recruit to nuclear foci, but the increase in
324 foci number ended abruptly at about 6 min. into interphase (Fig. 5 C and D). Interestingly the rate of increase
325 was also reduced, although the cause of this change is unclear we note that cycles 11 and 12 are also shortened

326 in *grp* embryos, which could result in a cumulative reduction in the amount of H3K9me2/3 carried over from
327 prior cycles. Thus, shortening interphase reduces the amount of heterochromatin formed.

328 Injection of *twine* (Cdc25) mRNA during cycle 13 can shorten interphase 14 and lead to an additional
329 mitosis by reintroducing CDK1 activity during a time when it is normally absent (Farrell et al. 2012). We found
330 that the extra mitosis induced in this way interrupted the accumulation of GFP-HP1a (Fig. 5E). Thus, premature
331 mitosis interferes with heterochromatin formation.

332 **DISCUSSION**

333 Histone modifications play a critical role in the epigenetic programs controlling development. The
334 chromatin in the early *Drosophila* embryo lacks many of these modifications and their restoration begins in an
335 unusual setting where cells divide remarkably quickly and in the absence of substantial transcription. The
336 reappearance of stable chromatin states coincides with the slowing of the cell cycle and the onset of major
337 transcription at the MBT. Here we have focused on the initial events controlling the de novo formation of the
338 heterochromatin. Using our new JabbaTrap method (Fig. 1), we showed that Eggless is the major H3K9
339 methyltransferase establishing heterochromatin domains in the embryo. Further using real time imaging, we
340 documented the early steps of heterochromatin formation and uncovered a close relationship between the
341 recruitment of Egg (Fig. 3E), the accumulation of H3K9me2/3-HP1a (Fig. 2A) and slowing of the cell cycle.
342 Experiments manipulating interphase duration indicate that this relationship is regulatory (Fig. 5). We propose
343 that the slowing of the cell cycle as the embryo approaches the MBT expands limited windows of opportunity
344 for Egg action and thereby times heterochromatin formation.

345 **JabbaTrapping – a new tool for inactivating maternal function**

346 The early embryo poses unique challenges to functional studies. The vast maternal supply present for
347 many gene products complicates traditional genetic analysis. Additionally, early embryonic events happen fast
348 so that methods that depend on destruction of RNA and protein must quickly destroy a large pool of target to
349 produce a phenotype. Our JabbaTrap approach can rapidly block maternal activities by mislocalizing target

350 proteins to lipid droplets (Fig. 1). Additionally, by establishing a transgenic system we deployed the JabbaTrap to
351 lipid droplets forming during oogenesis and mislocalized proteins during early embryogenesis. Interestingly, the
352 JabbaTrap also mislocalizes proteins that interact with the target (Fig. 4E) suggesting that it may be a useful
353 approach to inactivate entire nuclear protein complexes. In principle, the JabbaTrap could be applied to any
354 protein with a cognate nanobody, and we observed that the method successfully interferes with many different
355 nuclear functions. However, the function of cytoplasmic proteins might be less susceptible to inhibition by
356 localization to lipid droplets. The combination of nanobody based inactivation approaches and CRISPR-Cas9
357 gene editing to endogenously epitope tag proteins will allow easy functional studies in the future, and the
358 JabbaTrap fills a special need for such techniques in the dissection of early development.

359 **A new developmental model for the formation of heterochromatin**

360 The restoration of a more standard cell cycle regulation and timing at the MBT coincides with the
361 formation of mature heterochromatin. However, this is not a single change but a process involving a series of
362 precisely controlled events with the satellite DNA progressively acquiring different defining characteristics of
363 heterochromatin. Direct cytological examination demonstrated that satellite DNA is compacted as early as cycle
364 8 (Shermoen et al. 2010). Satellites begin exhibiting slight delays in replication time during cycles 10 through 13,
365 and then show major delays during S phase 14. This onset of late replication, and the consequent prolongation
366 of S phase 14 requires the action of the protein Rif1 (Seller and O'Farrell 2018). As the cell cycle slows during the
367 nuclear divisions leading up to the MBT, Egg deposits H3K9me2/3, which recruits HP1a to the heterochromatin.
368 By the end of cycle 14 the satellite sequences are stably marked by H3K9me2/3-HP1a, and they inherit or
369 maintain this modified state throughout development.

370 Although no obligate coupling is apparent, the embryonic cell cycle program controls the actions of both
371 Rif1 and Egg. Prior to the MBT high levels of cyclin-Cdk1 activity directly inhibit Rif1 by promoting its dissociation
372 from the satellite DNA thus ensuring short S phases (Seller and O'Farrell 2018). The cell cycle itself controls the
373 action of Eggless in two ways (Fig. 6). First, deposition of naïve histones during DNA replication halves the level

374 of histone modification in daughter nuclei. Prior studies have shown that the post S phase recovery of the level
375 of histone modification is slow (Alabert et al. 2015; Xu et al. 2012). Importantly, if a histone-modifying enzyme
376 does not double the amount of its product during a cell cycle then the level of modification will decrease over
377 time. Second, rapid cell cycles limit the opportunity for Egg action. Egg accumulates gradually at chromatin foci
378 during interphase, and accumulated Egg dissociates abruptly when chromosomes condense in preparation for
379 mitosis (Fig. 5A). As interphase extends in the approach to the MBT, both the amount of recruited Egg and its
380 residence time increase, leading to increased deposition of H3K9me2/3. For instance, during the 7-minute
381 interphase 11 Egg does recruit to chromatin, but its accumulation is minimal due to the rush to mitosis (Fig. 3E).
382 Only incremental increases in methyl marks occur prior to the much-elongated interphase 14. Indeed, the large
383 359 bp repeat only becomes stably associated with H3K9me2/3-HP1a during cycle 14 (Yuan and O'Farrell 2016),
384 and this association requires Egg (Fig. 2). Importantly, experimentally arresting the cell cycle in interphase
385 permitted continued accumulation of Egg and HP1a (Fig. 5B) while shortening interphase reduced the
386 recruitment of HP1a (Fig. 5 C and D). We conclude that the speed of early cell cycle limits the activity of
387 maternally provided Egg and that the schedule of cell cycle lengthening times the appearance of H3K9me2/3-
388 HP1a to give the observed weak accumulations in the later pre-MBT cycles and more fully elaborated
389 heterochromatin at the MBT (Fig 6).

390 Two recent studies reported that HP1 proteins display liquid like properties, and suggested that the
391 formation of heterochromatin domains depends on the ability of HP1 to phase separate (Larson et al. 2017;
392 Strom et al. 2017). In contrast, our previous observations (Shermoen et al. 2010; Yuan and O'Farrell 2016)
393 suggest that specific interactions trigger the deposition of heterochromatin marks on pre-existing compacted
394 foci of satellite sequences. Here we extend this view by uncovering a role for Egg in the early events of
395 heterochromatin formation. Among methyltransferases, Egg is uniquely required for initiation (Fig. 2).
396 Additionally, using live imaging we documented the first steps in the natural establishment of heterochromatin.
397 Early Egg accumulation localized to small puncta within larger foci of satellite sequences, suggesting a nucleation
398 process. Once recruited to chromatin, Egg deposits H3K9me2/3, and this mark seeds a domain of HP1a, which

399 then grows and spreads perhaps then utilizing HP1's liquid-like properties (Fig. 6). At least for some of the foci,
400 the small Egg focus does not seem to expand in concert with methylation and HP1a recruitment (Fig. 3A),
401 suggesting additional inputs.

402 We previously found that timely recruitment of ectopically introduced HP1a to the 359 satellite was
403 blocked by a mutation in its chromoshadow domain that prevents binding to a PxVxL motif (Yuan and O'Farrell,
404 2106), a seemingly unexpected dependency. This same study found that HP1a bearing a mutation blocking
405 K9me2/3 recognition (V26M mutant) still associated with this satellite, a finding that appears at odds with the
406 present finding that recruitment of HP1 to 359 requires the methyltransferase Egg. The meaning of these
407 observations is not clear. Perhaps dimerization or oligomerization allowed the ectopically introduced V26M
408 mutant to localize with endogenous wild-type HP1a that was recruited to foci of H3K9me2/3. Alternatively, Egg
409 might have methylation independent interactions that can recruit other proteins including HP1a in a
410 heterochromatin complex. The findings suggest that complex interactions guide maturation of heterochromatin
411 foci, and many details remain to be uncovered. Importantly, our present study identifies Egg as a key factor in
412 the earliest steps of this process.

413 Given that we observed recruitment of Egg to specific chromatin foci as early as cycle 10 (Fig. 3D) the
414 inputs specifying the future heterochromatic sequences must be present very early. However, we can currently
415 only speculate about how Egg is targeted. One attractive hypothesis is that specificity comes from maternally
416 deposited small RNAs that would recognize complementary nascent transcripts, much like the heterochromatin
417 machinery of *S. pombe* (Allshire and Madhani 2018). In support of this notion the recruitment of HP1a to the
418 359 repeat requires the maternal presence of this satellite indicating that this process is maternally guided (Yuan
419 and O'Farrell 2016). Additionally, Egg participates in the Piwi pathway and is directed to transposons in the
420 genome by complementary piRNAs, although the details of this mechanism are currently unclear (Sienski et al.
421 2015). A second possibility is that Egg binds to specific DNA binding proteins that act to specify its localization. A
422 family of DNA binding proteins known as KRAB-ZFP repressors target SetDB1 in mammals (Schultz et al. 2002).
423 While the KRAB family appears to be a tetrapod specific innovation, proteins recognizing specific satellite

424 repeats have been identified in *Drosophila*, and it remains a possibility that they recruit Egg to chromatin (Aulner
425 et al. 2002).

426 **Developmental specificity of methyltransferase action**

427 Development can employ the same protein for different purposes in different tissues and stages, and
428 Egg is prime example of this. Our results demonstrate that Egg plays a major role in the initial deposition of
429 heterochromatin in the embryo, but prior work had shown that loss of *egg* does not affect the association of
430 H3K9me2/3-HP1a at the chromocenter in larval polytene chromosomes (Seum et al. 2007a; Tzeng et al. 2007).
431 So Egg is critical for establishment, but not for the maintenance of heterochromatin. Interestingly, the reverse is
432 true for the methyltransferase Su(var)3-9. It makes only minimal contribution during initiation (Fig. 2B and C),
433 but then plays a dominant role later in development. We suggest that one key difference between these two
434 enzymes underlies this developmental specialization. Su(var)3-9, but not Egg, contains a chromodomain
435 allowing it to bind its own product making it ideal for maintenance (Schotta et al. 2002). This capacity allows for
436 positive feedback where prior methylation facilitates the modification of adjacent nucleosomes. In fission yeast
437 the chromodomain of the K9 methyltransferase Clr4 is critical for the spread and maintenance of domains of
438 H3K9me2/3 (Hall et al. 2002; Zhang et al. 2008; Al-Sady et al. 2013). Notably, a recent study in *C. elegans*
439 embryos uncovered that the SETDB1 methyltransferase (MET-2) is critical in this species for the formation of
440 heterochromatin, indicating that a special function for SETDB1 during initiation is conserved (Mutlu et al. 2018).

441 **Do rapid embryonic cell cycles wipe the slate clean during development?**

442 Although we have focused on the constitutive heterochromatin, our study could provide broader insight
443 into the regulation of histone modifying enzymes during development. In fact many other histone modifications
444 only appear at the MBT (Chen et al. 2013; Li et al. 2014), and direct examination of the enzymes installing these
445 marks during embryogenesis would be informative. We have emphasized the limitations that cell cycle speed
446 imposes on the restoration of the histone modifications, but we don't want to obscure what we think may be an
447 important benefit of these rapid divisions. Embryos inherit their genomes from their parents, and these parental

448 genomes come with parental chromatin modifications that are installed during gametogenesis (Loppin et al.
449 2005). The vast majority of animals develop externally from large eggs that begin with rapid cell divisions
450 without growth or transcriptional input. We suggest these fast cell cycles provided an ancestral mechanism to
451 reset the embryonic chromatin without the need for specific enzymes catalyzing the removal of histone
452 modifications. Multiple rounds of short S phases would dilute parental modifications, and brief interphases
453 would limit the action of maternally supplied chromatin modifying enzymes, which are present long before they
454 are needed. Developmental programs could then re-introduce these so-called epigenetics marks as the embryo
455 reaches the MBT, thereby coordinating the onset of zygotic transcription with the appearance of stable patterns
456 of histone modification. Notably, the situation in mammalian embryos is different with repressive modifications
457 appearing early during the cleavage stages (Fadloun et al. 2013). However, the evolution of placental
458 development restructured mammalian embryogenesis and the post-fertilization divisions are much slower and
459 transcription begins immediately. By controlling the speed of the embryonic cell cycle, development coordinates
460 the deposition of epigenetic modifications with the onset of zygotic transcription.

461 **METHODS**

462 *Fly stocks*

463 Stocks of *Drosophila melanogaster* were cultured on standard cornmeal-yeast media. The following previously
464 described stocks were used in this study: *w¹¹¹⁸* Canton-S (wild type), *His2Av-mRFP* (Bloomington stock number
465 23650), *EGFP-HP1a* (30561), *maternal tubulin-Gal4* (7063), *sfGFP-zelda* (M. Harrison), *ORC2-GFP*; *orc2^{1/y4}* (M.
466 Gossen), *G9a^{RG5}* (P. Spierer), *grp⁰⁶⁰³⁴*, *Su(var)3-9⁰⁶*, *Su(var)3-9¹⁷*, and *RIF1-EGFP*.

467 Embryo injections for the transgenic lines described in this study were done by Rainbow Transgenic Flies in
468 Camarillo, CA. PhiC31 mediated integration generated the JabbaTrap transgene *UASp-VhhGFP4-jabba-*
469 *VhhGFP4^{attP-9A}*. The following stocks were created using CRISPR-Cas9 gene editing: *sfGFP-Su(z)12*, *sfGFP-G9a*,
470 *EGFP-egg*, and *Halo-egg*. See Supplemental Fig. 1 for details of endogenous tagging. Following generation,

471 modified flies were crossed to our lab's wild type stock (w^{1118} *Canton-S*) for at least 5 generations. Plasmid DNA
472 and sequence files are available upon request.

473 *Protein purification*

474 Purified HP1a and TALE-light GFP/mCherry fusion proteins were described in previous studies (Shermoen et al.
475 2010; Yuan and O'Farrell 2016). Halo tagged 359 TALE-light protein was produced in BL21(DE3) *E. coli* cells.
476 Protein expression was induced by treating cultures with 0.5 mM IPTG overnight at room temperature. Bacteria
477 were lysed using B-PER supplemented with lysozyme, DNase I, and PMSF. TALE-light proteins were purified from
478 cleared lysate using Ni-NTA agarose in gravity flow columns. After 2 washes, 10 μ M of the halo ligand JF646 in
479 wash buffer was added to label the protein on column. Labeled proteins were eluted, dialyzed into 40 mM
480 HEPES (pH 7.4) with 150 mM KCl, and then concentrated by spin column. The concentrated eluate was
481 supplemented with glycerol to 10% and then snap frozen in liquid N₂.

482 *In vivo Halotag labeling of Drosophila embryos*

483 We adapted the embryo permeabilization method described in (Rand et al. 2010) to deliver the Halotag ligand
484 into the embryo, and permeabilization and labeling were conducted in a single step. Embryos were collected in
485 mesh baskets, dechorinated with 50% bleach, and then rinsed thoroughly with Embryo wash buffer and then
486 water. Using a brush, embryos were transferred to microfuge tubes with a 1:10 solution of Citrasolv containing 1
487 μ M JF549. The tubes were incubated on a nutator in the dark for 8 to 9 minutes. Embryos were then poured into
488 mesh baskets and cleaned thoroughly with wash buffer and water to remove excess detergent. Embryos were
489 then prepared for imaging following our normal protocol. Permeabilization was not always successful, but
490 embryos containing the dye could easily be identified microscopically.

491 *Immunoprecipitation and Western blotting*

492 Immunoprecipitation and western blotting were performed as described in (Seller and O'Farrell, 2018). The
493 following primary antibodies were used at a dilution of 1:1000: rabbit anti-GFP (ab290, Abcam, Cambridge,

494 United Kingdom) and rabbit anti-Wde (gift from A. Wodarz). A Goat anti-Rabbit HRP conjugated secondary
495 antibody (Biorad) was used at a dilution of 1:10,000.

496 *Embryo immunostaining*

497 Embryos were collected on grape agar plates, washed into mesh baskets and dechorinated in 50% bleach for 2
498 minutes. Embryos were then devitellenized and fixed in a 1:1 mixture of methanol-heptane, before storing in
499 methanol at -20°C. Embryos were gradually rehydrated in a series of increasing PTx:Methanol mixtures (1:3, 1:1,
500 3:1) before washing for 5 minutes in PTx (PBS with 0.1% Triton). Embryos were then blocked in PTx
501 supplemented with 5% Normal Donkey Serum and 0.2% Azide for 1 hour at room temperature. Blocked embryos
502 were then incubated with the primary antibody overnight at 4°C. The following primary antibodies were used:
503 rabbit anti-Wde at 1:500 (A. Wodarz), rabbit anti-H3K9me3 at 1:500, mouse anti-Ubx at 1:20 (DSHB FP3.38) and
504 mouse anti-HP1a at 1:100 (DSHB CA19). Embryos were then washed with PTx for three times 15 minutes each,
505 and then incubated with the appropriate fluorescently labeled secondary antibody (Molecular Probes) at 1:500
506 for 1 hour in the dark at room temperature. Embryos were then washed again with PTx for three times 15
507 minutes each. DAPI was added to the second wash. Finally, stained embryos were mounted on glass slides in
508 Fluoromount.

509 *Embryo microinjection and microscopy*

510 Embryo microinjections were performed as described in (Farrell et al. 2012). JabbaTrap and Cdc25 (*twine*)
511 mRNAs were synthesized using the CellScript T7 mRNA production system and injected at a concentration of 600
512 ng/μl. dsRNA against the cyclins A, B, and B3 was prepared as described in (McCleland and O'Farrell 2008).
513 Imaging was performed using a spinning disk confocal microscope as described in (Seller and O'Farrell 2018).
514 Image processing and analysis were done using Volocity (Perkin Elmer) and ImageJ. Unless otherwise noted, all
515 images are presented as z-stack projections.

516

517 **Acknowledgements**

518 We thank past and present members of the O'Farrell laboratory, especially Kai Yuan, Antony Shermoen, and
519 Mark McCleland for guidance and reagents. We also thank Anna Holman for early work on this project. Hiroshi
520 Kimura generously provided labeled Fab reagents for H3K9me2. Luke Lavis generously provided halotag ligands
521 labeled with Janelia Fluorescent dyes. The Bloomington Stock Center and the *Drosophila* community provided
522 important reagents and fly stocks throughout this work.

523 **Author Contributions**

524 **Charles Seller:** Conceptualization, Investigation, Writing.

525 **Chun-Yi Cho:** Investigation, Editing.

526 **Patrick O'Farrell:** Conceptualization, Writing, Supervision.

527 **References**

528 Alabert C, Barth TK, Reverón-Gómez N, Sidoli S, Schmidt A, Jensen ON, Imhof A, Groth A. 2015. Two distinct
529 modes for propagation of histone PTMs across the cell cycle. *Genes Dev* **29**: 585–590.

530 Allshire RC, Madhani HD. 2018. Ten principles of heterochromatin formation and function. *Nature Reviews
531 Molecular Cell Biology* **19**: 229–244.

532 Al-Sady B, Madhani HD, Narlikar GJ. 2013. Division of Labor between the Chromodomains of HP1 and Suv39
533 Methylase Enables Coordination of Heterochromatin Spread. *Molecular Cell* **51**: 80–91.

534 Aulner N, Monod C, Mandicourt G, Jullien D, Cuvier O, Sall A, Janssen S, Laemmli UK, Käs E. 2002. The AT-Hook
535 Protein D1 Is Essential for *Drosophila melanogaster* Development and Is Implicated in Position-Effect
536 Variegation. *Molecular and Cellular Biology* **22**: 1218–1232.

537 Baldinger T, Gossen M. 2009. Binding of *Drosophila* Orc Proteins to Anaphase Chromosomes Requires Cessation
538 of Mitotic Cyclin-Dependent Kinase Activity. *Molecular and Cellular Biology* **29**: 140–149.

539 Birve A, Sengupta AK, Beuchle D, Larsson J, Kennison JA, Rasmuson-Lestander Å, Müller J. 2001. Su(z)12, a novel
540 *Drosophila* Polycomb group gene that is conserved in vertebrates and plants. *Development* **128**: 3371–
541 3379.

542 Brower-Toland B, Riddle NC, Jiang H, Huisenga KL, Elgin SCR. 2009. Multiple SET Methyltransferases Are Required
543 to Maintain Normal Heterochromatin Domains in the Genome of *Drosophila melanogaster*. *Genetics*
544 **181**: 1303–1319.

545 Brown SW. 1966. Heterochromatin. *Science* **151**: 417–425.

546 Chen K, Johnston J, Shao W, Meier S, Staber C, Zeitlinger J. 2013. A global change in RNA polymerase II pausing
547 during the *Drosophila* midblastula transition. *eLife* **2**: e00861.

548 Clough E, Moon W, Wang S, Smith K, Hazelrigg T. 2007. Histone methylation is required for oogenesis in
549 *Drosophila*. *Development* **134**: 157–165.

550 Clough E, Tedeschi T, Hazelrigg T. 2014. Epigenetic regulation of oogenesis and germ stem cell maintenance by
551 the *Drosophila* histone methyltransferase Eggless/dSetDB1. *Developmental Biology* **388**: 181–191.

552 Eissenberg JC, Elgin SCR. 2014. HP1a: a structural chromosomal protein regulating transcription. *Trends in*
553 *Genetics* **30**: 103–110.

554 Eissenberg JC, James TC, Foster-Hartnett DM, Hartnett T, Ngan V, Elgin SC. 1990. Mutation in a heterochromatin-
555 specific chromosomal protein is associated with suppression of position-effect variegation in *Drosophila*
556 *melanogaster*. *PNAS* **87**: 9923–9927.

557 Elgin SCR, Reuter G. 2013. Position-Effect Variegation, Heterochromatin Formation, and Gene Silencing in
558 *Drosophila*. *Cold Spring Harb Perspect Biol* **5**: a017780.

559 Fadloun A, Eid A, Torres-Padilla M-E. 2013. Chapter One - Mechanisms and Dynamics of Heterochromatin
560 Formation During Mammalian Development: Closed Paths and Open Questions. In *Current Topics in*
561 *Developmental Biology* (ed. E. Heard), Vol. 104 of *Epigenetics and Development*, pp. 1–45.

562 Farrell JA, O'Farrell PH. 2014. From Egg to Gastrula: How the Cell Cycle Is Remodeled During the *Drosophila* Mid-
563 Blastula Transition. *Annual Review of Genetics* **48**: 269–294.

564 Farrell JA, Shermoen AW, Yuan K, O'Farrell PH. 2012. Embryonic onset of late replication requires Cdc25 down-
565 regulation. *Genes Dev* **26**: 714–725.

566 Grimm JB, English BP, Chen J, Slaughter JP, Zhang Z, Revyakin A, Patel R, Macklin JJ, Normanno D, Singer RH, et
567 al. 2015. A general method to improve fluorophores for live-cell and single-molecule microscopy. *Nature*
568 *Methods* **12**: 244–250.

569 Hall IM, Shankaranarayana GD, Noma K, Ayoub N, Cohen A, Grewal SIS. 2002. Establishment and Maintenance of
570 a Heterochromatin Domain. *Science* **297**: 2232–2237.

571 Haruki H, Nishikawa J, Laemmli UK. 2008. The Anchor-Away Technique: Rapid, Conditional Establishment of
572 Yeast Mutant Phenotypes. *Molecular Cell* **31**: 925–932.

573 Hayashi-Takanaka Y, Yamagata K, Wakayama T, Stasevich TJ, Kainuma T, Tsurimoto T, Tachibana M, Shinkai Y,
574 Kurumizaka H, Nozaki N, et al. 2011. Tracking epigenetic histone modifications in single cells using Fab-
575 based live endogenous modification labeling. *Nucleic Acids Res* **39**: 6475–6488.

576 Janssen A, Colmenares SU, Karpen GH. 2018. Heterochromatin: Guardian of the Genome. *Annual Review of Cell*
577 and *Developmental Biology* **34**: 265–288.

578 Koch CM, Honemann-Capito M, Egger-Adam D, Wodarz A. 2009. Windei, the *Drosophila* Homolog of
579 mAM/MCAF1, Is an Essential Cofactor of the H3K9 Methyl Transferase dSETDB1/Eggless in Germ Line
580 Development. *PLOS Genetics* **5**: e1000644.

581 Larson AG, Elnatan D, Keenen MM, Trnka MJ, Johnston JB, Burlingame AL, Agard DA, Redding S, Narlikar GJ.
582 2017. Liquid droplet formation by HP1 α suggests a role for phase separation in heterochromatin. *Nature*
583 **547**: 236–240.

584 Li X-Y, Harrison MM, Villalta JE, Kaplan T, Eisen MB. 2014. Establishment of regions of genomic activity during
585 the Drosophila maternal to zygotic transition. *eLife* **3**: e03737.

586 Li Z, Thiel K, Thul PJ, Beller M, Kühnlein RP, Welte MA. 2012. Lipid Droplets Control the Maternal Histone Supply
587 of Drosophila Embryos. *Current Biology* **22**: 2104–2113.

588 Liang H-L, Nien C-Y, Liu H-Y, Metzstein MM, Kirov N, Rushlow C. 2008. The zinc-finger protein Zelda is a key
589 activator of the early zygotic genome in *Drosophila*. *Nature* **456**: 400–403.

590 Loppin B, Bonnefoy E, Anselme C, Laurençon A, Karr TL, Couble P. 2005. The histone H3.3 chaperone HIRA is
591 essential for chromatin assembly in the male pronucleus. *Nature* **437**: 1386–1390.

592 McCleland ML, O'Farrell PH. 2008. RNAi of Mitotic Cyclins in Drosophila Uncouples the Nuclear and Centrosome
593 Cycle. *Current Biology* **18**: 245–254.

594 Mis J, Ner SS, Grigliatti TA. 2006. Identification of three histone methyltransferases in *Drosophila*: dG9a is a
595 suppressor of PEV and is required for gene silencing. *Mol Genet Genomics* **275**: 513–526.

596 Mutlu B, Chen H-M, Moresco JJ, Orello BD, Yang B, Gaspar JM, Keppler-Ross S, Yates JR, Hall DH, Maine EM, et al.
597 2018. Regulated nuclear accumulation of a histone methyltransferase times the onset of
598 heterochromatin formation in *C. elegans* embryos. *Science Advances* **4**: eaat6224.

599 Penke TJR, McKay DJ, Strahl BD, Matera AG, Duronio RJ. 2016. Direct interrogation of the role of H3K9 in
600 metazoan heterochromatin function. *Genes Dev* **30**: 1866–1880.

601 Penke TJR, McKay DJ, Strahl BD, Matera AG, Duronio RJ. 2018. Functional Redundancy of Variant and Canonical
602 Histone H3 Lysine 9 Modification in *Drosophila*. *Genetics* **208**: 229–244.

603 Rand MD, Kearney AL, Dao J, Clason T. 2010. Permeabilization of *Drosophila* embryos for introduction of small
604 molecules. *Insect Biochemistry and Molecular Biology* **40**: 792–804.

605 Rangan P, Malone CD, Navarro C, Newbold SP, Hayes PS, Sachidanandam R, Hannon GJ, Lehmann R. 2011. piRNA
606 Production Requires Heterochromatin Formation in *Drosophila*. *Current Biology* **21**: 1373–1379.

607 Riddle NC, Jung YL, Gu T, Alekseyenko AA, Asker D, Gui H, Kharchenko PV, Minoda A, Plachetka A, Schwartz YB,
608 et al. 2012. Enrichment of HP1 α on *Drosophila* Chromosome 4 Genes Creates an Alternate Chromatin
609 Structure Critical for Regulation in this Heterochromatic Domain. *PLOS Genetics* **8**: e1002954.

610 Rothbauer U, Zolghadr K, Muyldermans S, Schepers A, Cardoso MC, Leonhardt H. 2008. A Versatile Nanotrap for
611 Biochemical and Functional Studies with Fluorescent Fusion Proteins. *Molecular & Cellular Proteomics* **7**:
612 282–289.

613 Schotta G, Ebert A, Krauss V, Fischer A, Hoffmann J, Rea S, Jenuwein T, Dorn R, Reuter G. 2002. Central role of
614 Drosophila SU(VAR)3–9 in histone H3-K9 methylation and heterochromatic gene silencing. *The EMBO
615 Journal* **21**: 1121–1131.

616 Schultz DC, Ayyanathan K, Negorev D, Maul GG, Rauscher FJ. 2002. SETDB1: a novel KAP-1-associated histone
617 H3, lysine 9-specific methyltransferase that contributes to HP1-mediated silencing of euchromatic genes
618 by KRAB zinc-finger proteins. *Genes Dev* **16**: 919–932.

619 Seller CA, O'Farrell PH. 2018. Rif1 prolongs the embryonic S phase at the Drosophila mid-blastula transition.
620 *PLOS Biology* **16**: e2005687.

621 Seum C, Bontron S, Reo E, Delattre M, Spierer P. 2007a. Drosophila G9a Is a Nonessential Gene. *Genetics* **177**:
622 1955–1957.

623 Seum C, Reo E, Peng H, Ilii FJR, Spierer P, Bontron S. 2007b. Drosophila SETDB1 Is Required for Chromosome 4
624 Silencing. *PLOS Genetics* **3**: e76.

625 Shermoen AW, McCleland ML, O'Farrell PH. 2010. Developmental Control of Late Replication and S Phase
626 Length. *Current Biology* **20**: 2067–2077.

627 Shermoen AW, O'Farrell PH. 1991. Progression of the cell cycle through mitosis leads to abortion of nascent
628 transcripts. *Cell* **67**: 303–310.

629 Sibon OCM, Stevenson VA, Theurkauf WE. 1997. DNA-replication checkpoint control at the *Drosophila*
630 midblastula transition. *Nature* **388**: 93–97.

631 Sienski G, Batki J, Senti K-A, Dönertas D, Tirian L, Meixner K, Brennecke J. 2015. Silencio/CG9754 connects the
632 Piwi–piRNA complex to the cellular heterochromatin machinery. *Genes Dev* **29**: 2258–2271.

633 Strom AR, Emelyanov AV, Mir M, Fyodorov DV, Darzacq X, Karpen GH. 2017. Phase separation drives
634 heterochromatin domain formation. *Nature* **547**: 241–245.

635 Strong I, Yuan K, O'Farrell PH. 2017. Interphase-Arrested Drosophila Embryos Initiate Mid-Blastula Transition At
636 A Low Nuclear-Cytoplasmic Ratio. *bioRxiv* 143719.

637 Tschiersch B, Hofmann A, Krauss V, Dorn R, Korge G, Reuter G. 1994. The protein encoded by the Drosophila
638 position-effect variegation suppressor gene Su(var)3-9 combines domains of antagonistic regulators of
639 homeotic gene complexes. *EMBO J* **13**: 3822–3831.

640 Tzeng T-Y, Lee C-H, Chan L-W, Shen C-KJ. 2007. Epigenetic regulation of the Drosophila chromosome 4 by the
641 histone H3K9 methyltransferase dSETDB1. *PNAS* **104**: 12691–12696.

642 Wang H, An W, Cao R, Xia L, Erdjument-Bromage H, Chatton B, Tempst P, Roeder RG, Zhang Y. 2003. mAM
643 Facilitates Conversion by ESET of Dimethyl to Trimethyl Lysine 9 of Histone H3 to Cause Transcriptional
644 Repression. *Molecular Cell* **12**: 475–487.

645 Wang X, Pan L, Wang S, Zhou J, McDowell W, Park J, Haug J, Staehling K, Tang H, Xie T. 2011. Histone H3K9
646 Trimethylase Eggless Controls Germline Stem Cell Maintenance and Differentiation. *PLOS Genetics* **7**:
647 e1002426.

648 Welte MA. 2015. As the fat flies: The dynamic lipid droplets of Drosophila embryos. *Biochimica et Biophysica
649 Acta (BBA) - Molecular and Cell Biology of Lipids* **1851**: 1156–1185.

650 Xu M, Wang W, Chen S, Zhu B. 2012. A model for mitotic inheritance of histone lysine methylation. *EMBO
651 reports* **13**: 60–67.

652 Yu Y, Gu J, Jin Y, Luo Y, Preall JB, Ma J, Czech B, Hannon GJ. 2015. Panoramix enforces piRNA-dependent
653 cotranscriptional silencing. *Science* **350**: 339–342.

654 Yuan K, O'Farrell PH. 2016. TALE-light imaging reveals maternally guided, H3K9me2/3-independent emergence
655 of functional heterochromatin in *Drosophila* embryos. *Genes Dev* **30**: 579–593.

656 Yuan K, Seller CA, Shermoen AW, O'Farrell PH. 2016. Timing the *Drosophila* Mid-Blastula Transition: A Cell Cycle-
657 Centered View. *Trends in Genetics* **32**: 496–507.

658 Yuan K, Shermoen AW, O'Farrell PH. 2014. Illuminating DNA replication during *Drosophila* development using
659 TALE-lights. *Current Biology* **24**: R144–R145.

660 Zhang K, Mosch K, Fischle W, Grewal SIS. 2008. Roles of the Clr4 methyltransferase complex in nucleation,
661 spreading and maintenance of heterochromatin. *Nature Structural & Molecular Biology* **15**: 381–388.

662

663

664

665

666

667

668

669

670

671

672

673

674

675

676

677

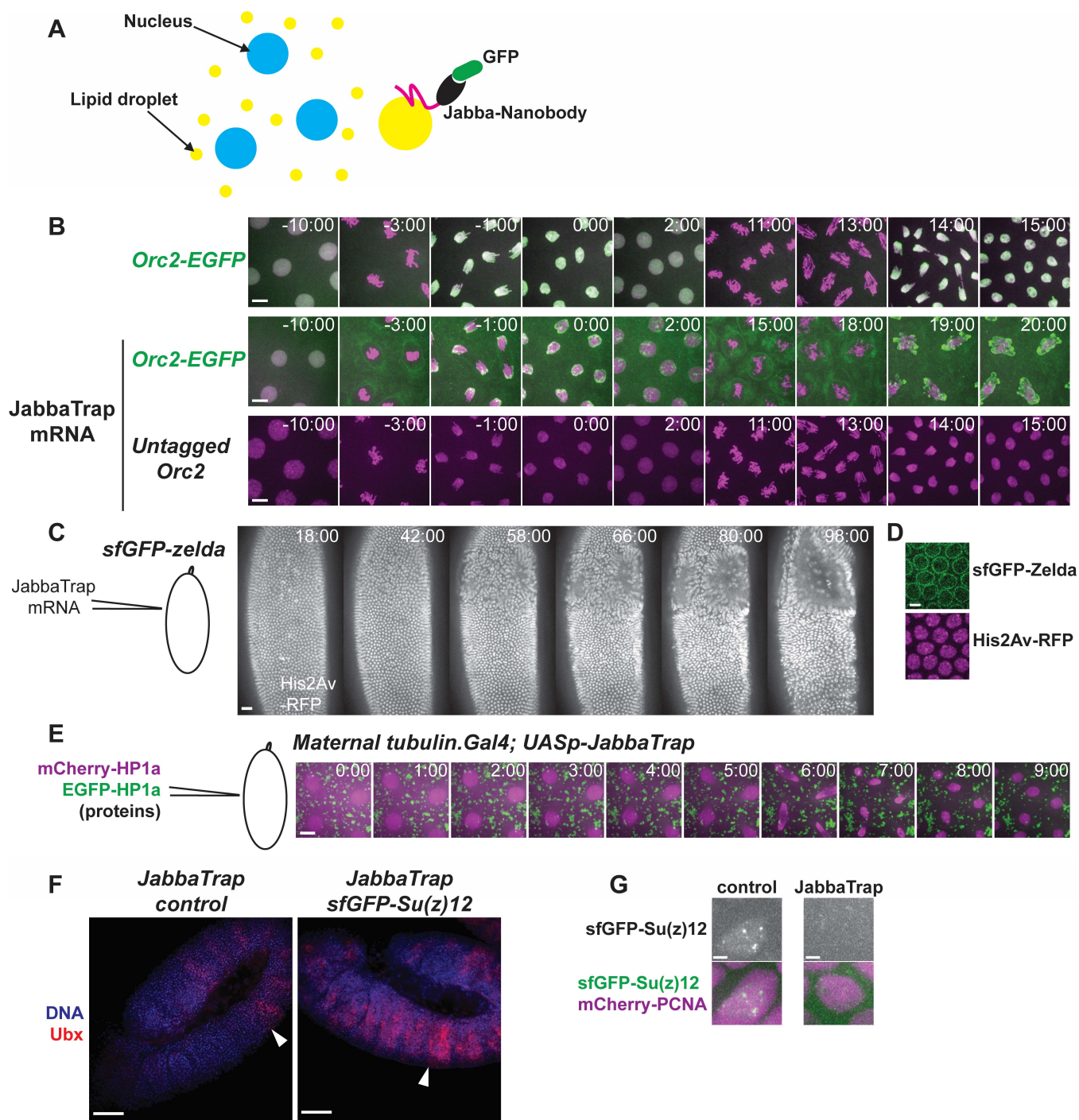
678

679

680

681

682



684 **Fig. 1** JabbaTrap rapidly mis-localizes and blocks nuclear proteins in the embryo.

685

686

687

688

689

690

691 **Fig. 1 JabbaTrap rapidly mis-localizes and blocks nuclear proteins in the embryo.**

692 **A)** Schematic of the JabbaTrap technique. Lipid droplets (yellow circles), which serve as storage organelles, are
693 distributed throughout the cytoplasm of the syncytial embryo. Ectopic expression of Jabba fused to an anti-GFP
694 nanobody traps GFP tagged proteins on lipid droplets. **B)** The Jabbatrap mislocalizes Orc2 and blocks DNA
695 replication. Stills from live imaging of embryos of the indicated genotype after injection of Cy5 labeled histone
696 proteins alone or together with JabbaTrap mRNA. Top row, Orc2-GFP embryos injected with labeled histones
697 (shown in magenta) only. Orc2 (shown in green) rapidly binds to the anaphase chromosomes (-1:00) and
698 remains nuclear during the subsequent interphase. In Orc2-GFP embryos injected with both labeled histones
699 and Jabbatrap message (middle row), Orc2 is prevented from binding to the chromosomes and mislocalized to
700 both the reforming nuclear envelope and to puncta in the cytoplasm. Anaphase bridging occurs in the following
701 mitosis (19:00). Bottom row, wildtype embryos injected with both Cy5-histones and JabbaTrap mRNA undergo
702 normal mitotic cycles. Scale bar is 3 μ m. See Supplemental Movie 1. **C)** Stills from live imaging following His2Av-
703 RFP in an sfGFP-Zelda embryo injected with JabbaTrap mRNA. Nuclei near the injection site failed to cellularize
704 and collapsed out of the cortical layer. Scale bar is 10 μ m and the start of cycle 14 is set as 0:00. **D)** Single z plane
705 showing the mislocalization of sfGFP-Zelda by expression of JabbaTrap mRNA. Scale bar is 2 μ m. **E)** Co-injection
706 of mCherry-HP1a and GFP-HP1a into an embryo from mothers expressing transgenic JabbaTrap during
707 oogenesis. Scale bar is 4 μ m. **F)** JabbaTrap expression blocks sfGFP-Su(z)12 leading to derepression of the
708 homeotic protein Ubx. The white arrowhead indicates the wild-type anterior border of Ubx expression. Embryos
709 stained with DAPI (blue) and anti-Ubx (red). Scale bar is 25 μ m. **(G)** Control or JabbaTrap expressing sfGFP-
710 Su(z)12 embryos injected with mCherry-PCNA to label the nucleus. The JabbaTrap mislocalizes Su(z)12 to the
711 cytoplasm. Scale bar is 1 μ m.

712

713

714

715

716

717

718

719

720

721

722

723

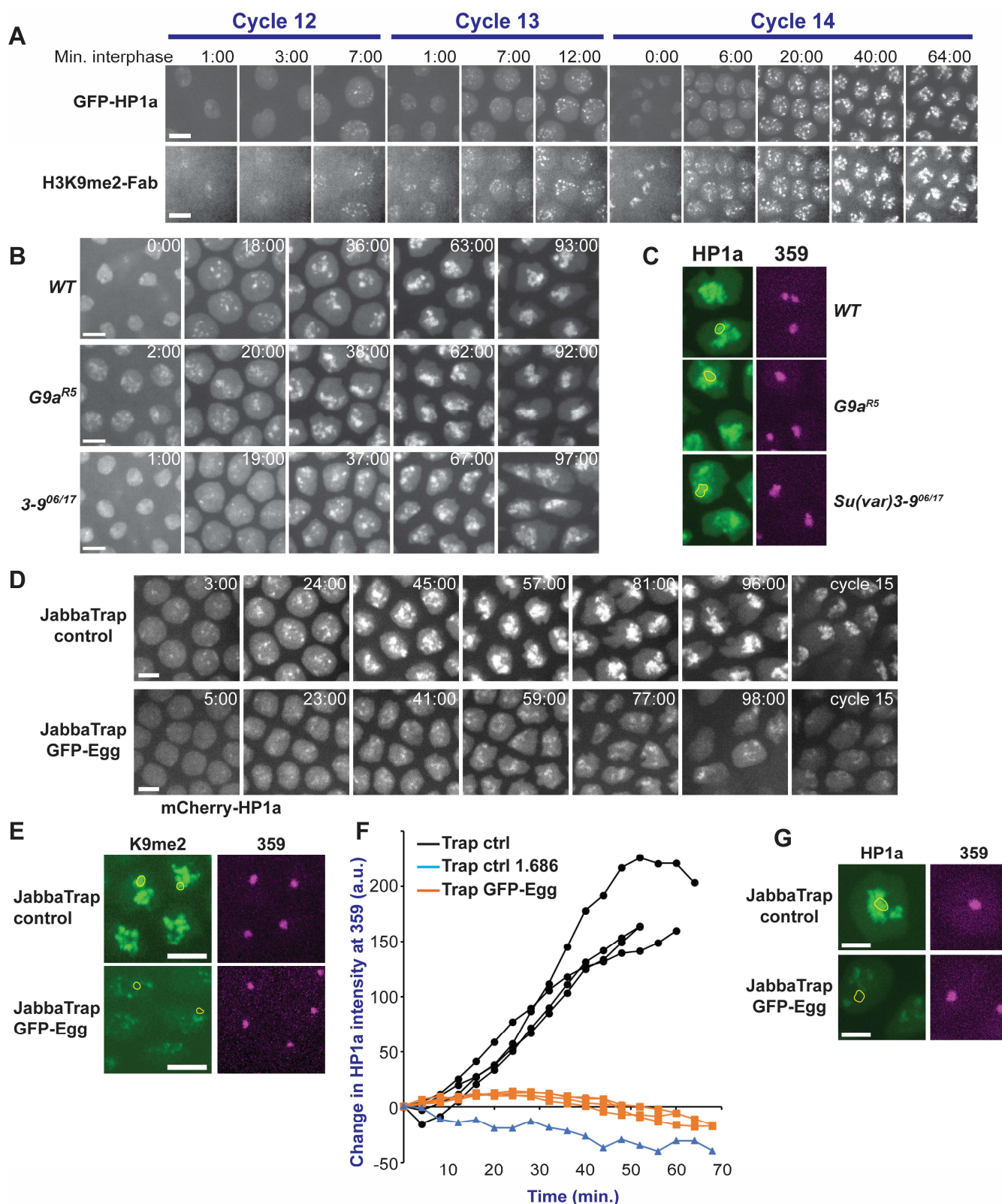
724

725

726

727

728



729

730 **Fig. 2 Eggless is required for the embryonic establishment of heterochromatin.**

731

732

733 **Fig. 2 Eggless is required for the embryonic establishment of heterochromatin.**

734 **A)** Progressive accumulation of H3K9me2-HP1a in the early embryo. Selected stills from live imaging over 3 cell
735 cycles of GFP-HP1a embryos injected with Cy5 labeled H3K9me2 Fab fragment. Scale bar is 3 μ m. See
736 Supplemental Movie 2. **(B,C)** G9a and Su(var)3-9 are not required for the establishment of heterochromatin. **B)**
737 Selected stills from live imaging of embryos of the indicated genotype injected with mCherry-HP1a protein. The
738 beginning of interphase 14 was set as 0:00. The scale bar is 2 μ m. **C)** Stills of live embryos of the indicated
739 genotype injected with GFP-HP1a and 359-TALE-mCherry. The location of 359 is outlined in yellow on the HP1a
740 channel. Images were acquired approximately 1 hour into interphase 14. **(D-G)** JabbaTrapping Egg blocks the
741 embryonic onset of H3K9me2-HP1. **D)** Live imaging of mCherry-HP1a injected into wildtype control or GFP-Egg
742 embryos following maternal expression of the JabbaTrap. Mislocalization of Egg significantly reduced and
743 delayed the accumulation of HP1a at the heterochromatin. The start of interphase 14 was set as 0:00. The scale
744 bar is 3 μ m. Compare Supplemental Movies 3 and 4. **E)** Stills from live embryos of the indicated genotype
745 injected with Cy5 labeled H3K9me2 Fab fragments and 359-TALE-mCherry. The position of 359 is outlined in
746 yellow on the H3K9me2 channel. Images were acquired approximately 1 hour into interphase 14. Scale bar is 2
747 μ m. **F)** Plot of the change in mCherry-HP1a fluorescence at the 359 bp repeat over time during interphase 14.
748 The 1.686 satellite, which does not recruit HP1a, serves as a negative control. Each line represents a different
749 embryo, where fluorescence was measured in over 20 nuclei per embryo and the mean average for each time
750 point was calculated. **G)** Stills from live embryos of the indicated genotype injected with mCherry-HP1a and 359-
751 TALE-HaloJF646. The position of 359 is outlined in yellow on the HP1a channel. Embryos are approximately 80
752 minutes into interphase 14, during cephalic furrow formation. The scale bar is 1 μ m.

753

754

755

756

757

758

759

760

761

762

763

764

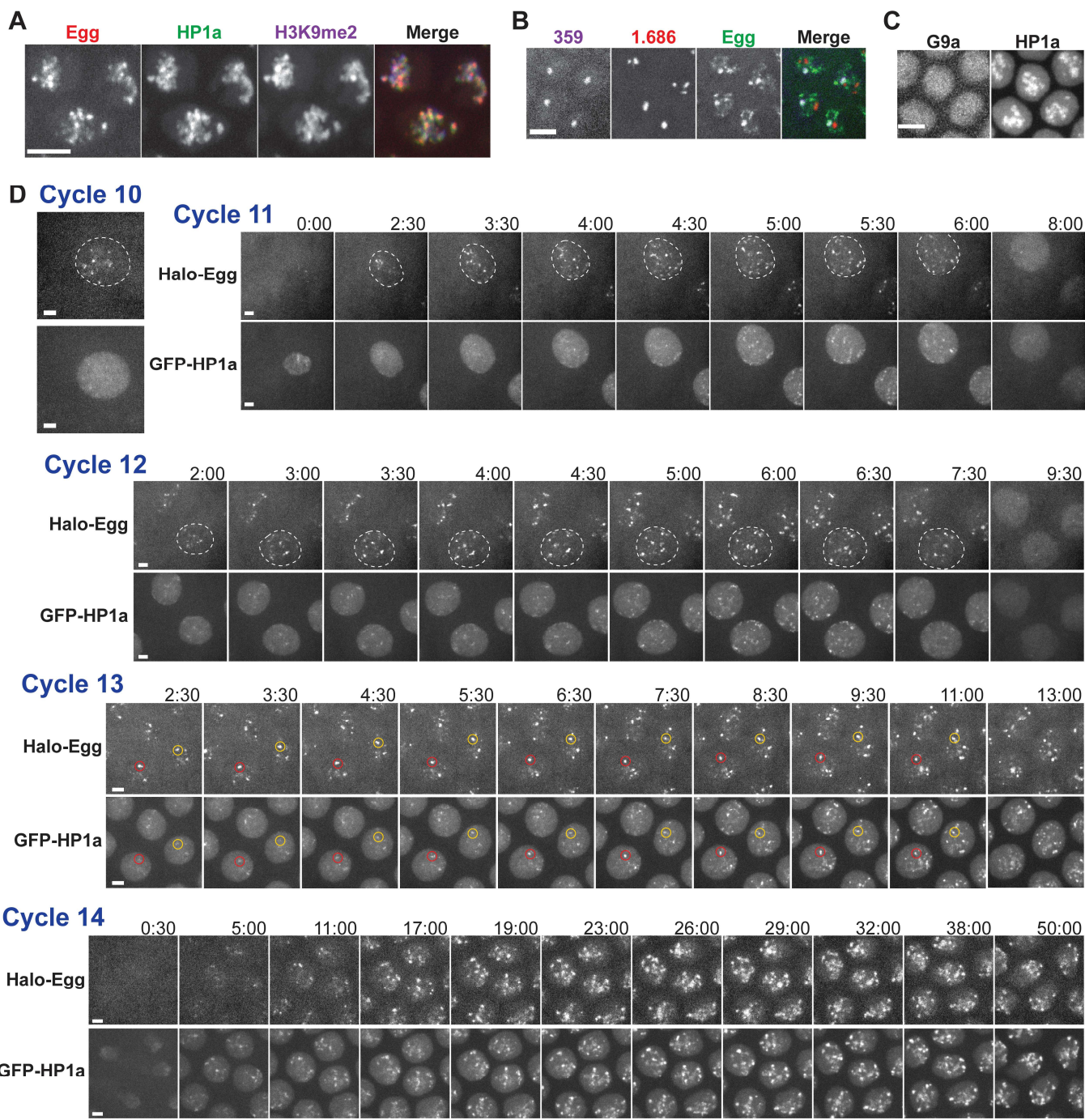
765

766

767

768

769



770

771 **Fig. 3 localization and dynamics of Egg during the establishment of heterochromatin.**

772

773

774

775

776

777

778 **Fig. 3 localization and dynamics of Egg during the establishment of heterochromatin.**

779 **A)** Confocal micrographs of a cycle 14 Halo(JF549)-Egg embryo injected with GFP-HP1a and Cy5 labeled
780 H3K9me2 Fab. Scale bar 2 μ m. **B)** Confocal micrograph of a cycle 14 GFP-Egg embryo injected with Halo(JF646)-
781 359 and mCherry-1.686 TALE-Lights. Scale bar is 2 μ m. **C)** Confocal micrographs of a live sfGFP-G9a embryo
782 injected with mCherry-HP1a show that G9a does not localize to heterochromatin. Images were acquired
783 approximately 50 min. into interphase 14. Scale bar 2 μ m. **D)** Selected stills from live imaging of Halo(JF549)-Egg
784 and GFP-HP1a during cycles 10-14 as interphase duration naturally extends. The recorded cycle is indicated
785 above the micrographs. Egg accumulates at multiple bright foci in the interphase nucleus (denoted in dashed
786 white line). Note that the recruitment of Egg precedes that of HP1a during development and during the cell
787 cycle. Longer interphases permit increased accumulation of Egg on chromatin. Yellow and red circles in cycle 13
788 records track the fate of two foci of Egg and the corresponding locations in the HP1a channel. Each cell cycle was
789 recorded from a different Halo-Egg embryo labeled with JF549 and the beginning of interphase was set as 0:00.
790 Scale bars are 1 μ m. See Supplemental Movie 5.

791

792

793

794

795

796

797

798

799

800

801

802

803

804

805

806

807

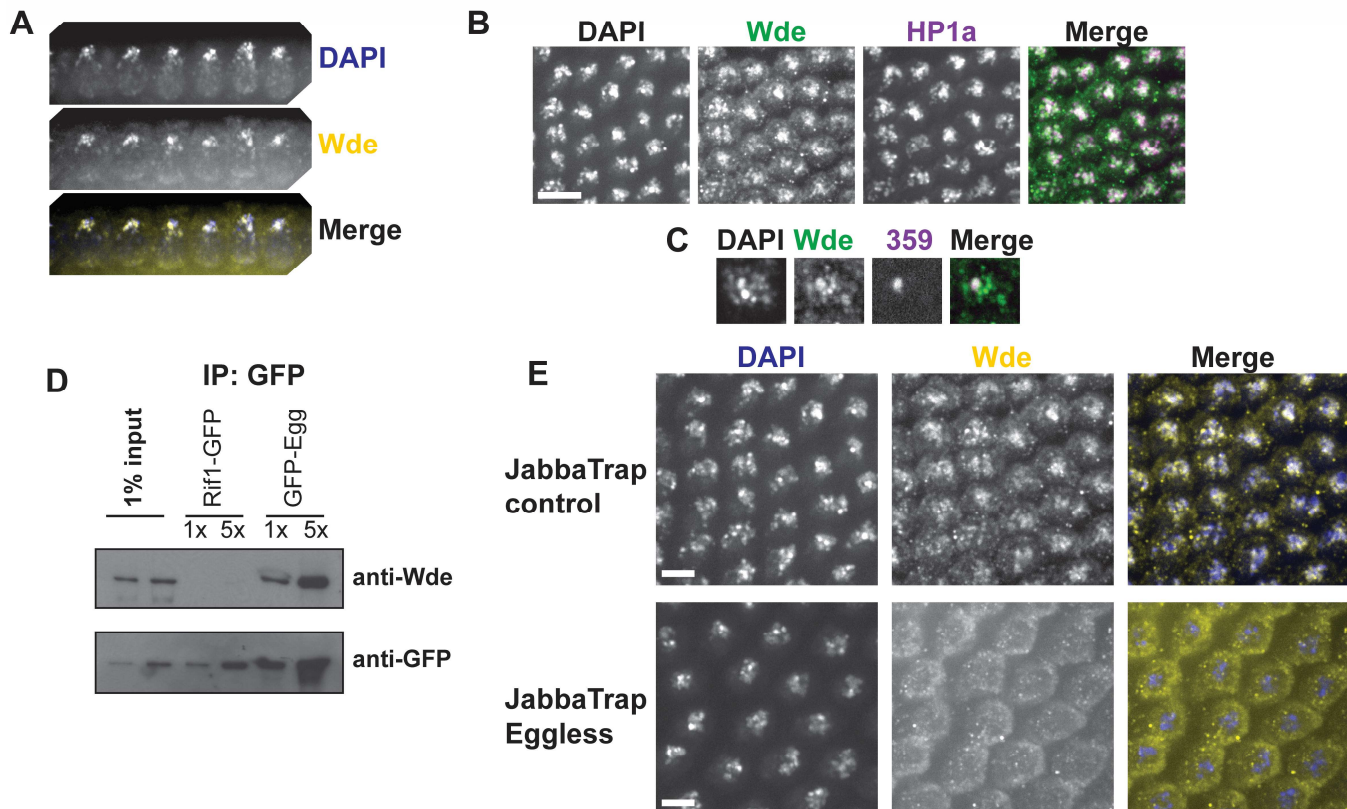
808

809

810

811

812



813

814 **Fig. 4** Windei, a cofactor of Egg, localizes to the heterochromatin in the embryo and interacts with Egg.

815 (A-C) Wde is enriched at the constitutive heterochromatin in early embryos. **A)** Co-localization of Wde with the
816 DAPI intense apical portion of the nucleus in fixed embryos. **B)** Cycle 14 embryos immunostained for HP1a and
817 Wde. Scale bar is 5 μ m. **C)** Fixed cycle 14 embryo stained for Wde and with a TALE-light recognizing the 359 bp
818 repeat. **D)** GFP-Egg was immunoprecipitated from 1 to 3 hour old embryos and analyzed by western blotting.
819 Wde interacts with Egg in the early embryo. **E)** Fixed embryos expressing the JabbaTrap in either a control or
820 GFP-Egg background were immunostained for Wde. Wde is mislocalized to the cytoplasm when GFP-Egg is
821 JabbaTrapped. Scale bar is 3 μ m.

822

823

824

825

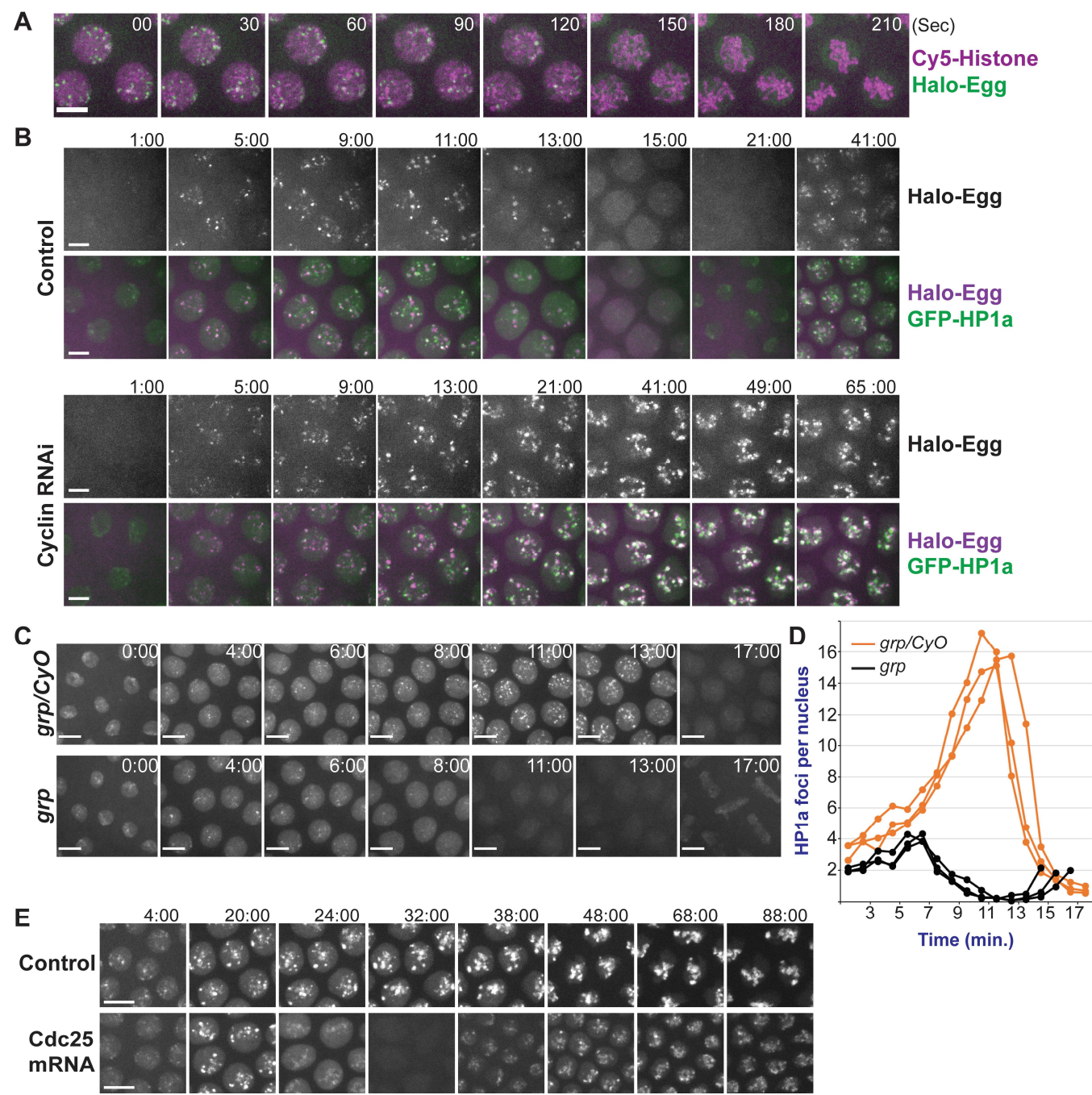
826

827

828

829

830



831

832 **Fig. 5 Interphase duration limits the establishment of heterochromatin.**

833

834

835

836

837

838

839 **Fig. 5 Interphase duration limits the establishment of heterochromatin.**

840 **A)** Selected stills from live imaging of Halo-Egg (shown in green) embryos injected with Cy5 labeled Histone
841 proteins (shown in magenta). Egg dissociates from the chromatin upon mitotic chromosome condensation (150
842 sec.). Scale bar is 3 μ m. See Supplemental Movie 6. **B)** Arresting the cell cycle in interphase 13 permits continued
843 accumulation of Egg and HP1a at heterochromatin. Embryos were filmed by confocal microscopy after injection
844 of buffer or dsRNA against cyclins A, B, and B3. Scale bar is 2 μ m and the beginning of cycle 13 was set as 0:00.
845 See Supplemental Movie 7. **(C-E)** Shortening interphase duration reduces HP1a accumulation. **C)** Stills from
846 confocal microscopy tracking GFP-HP1a in embryos laid from mothers either heterozygous or homozygous for
847 *grp*. Note that *grp* embryos enter mitosis 13 before completing S phase leading to anaphase bridges (17:00).
848 Scale bar is 4 μ m and the start of interphase 13 was set as 0:00. **D)** Plot of the average number of HP1a foci per
849 nucleus over time in control embryos (orange) or *grp* embryos (black). Each line represents data from a different
850 embryo, and foci of GFP-HP1a were counted in approximately 15 nuclei per embryo. **E)** Inducing an early mitosis
851 14 by expression of twine (cdc25) interrupts heterochromatin formation. Embryos expressing GFP-HP1a were
852 filmed following injection of twine mRNA during cycle 13. Scale bar is 3 μ m and the beginning of cycle 14 was set
853 as 0:00.

854

855

856

857

858

859

860

861

862

863

864

865

866

867

868

869

870

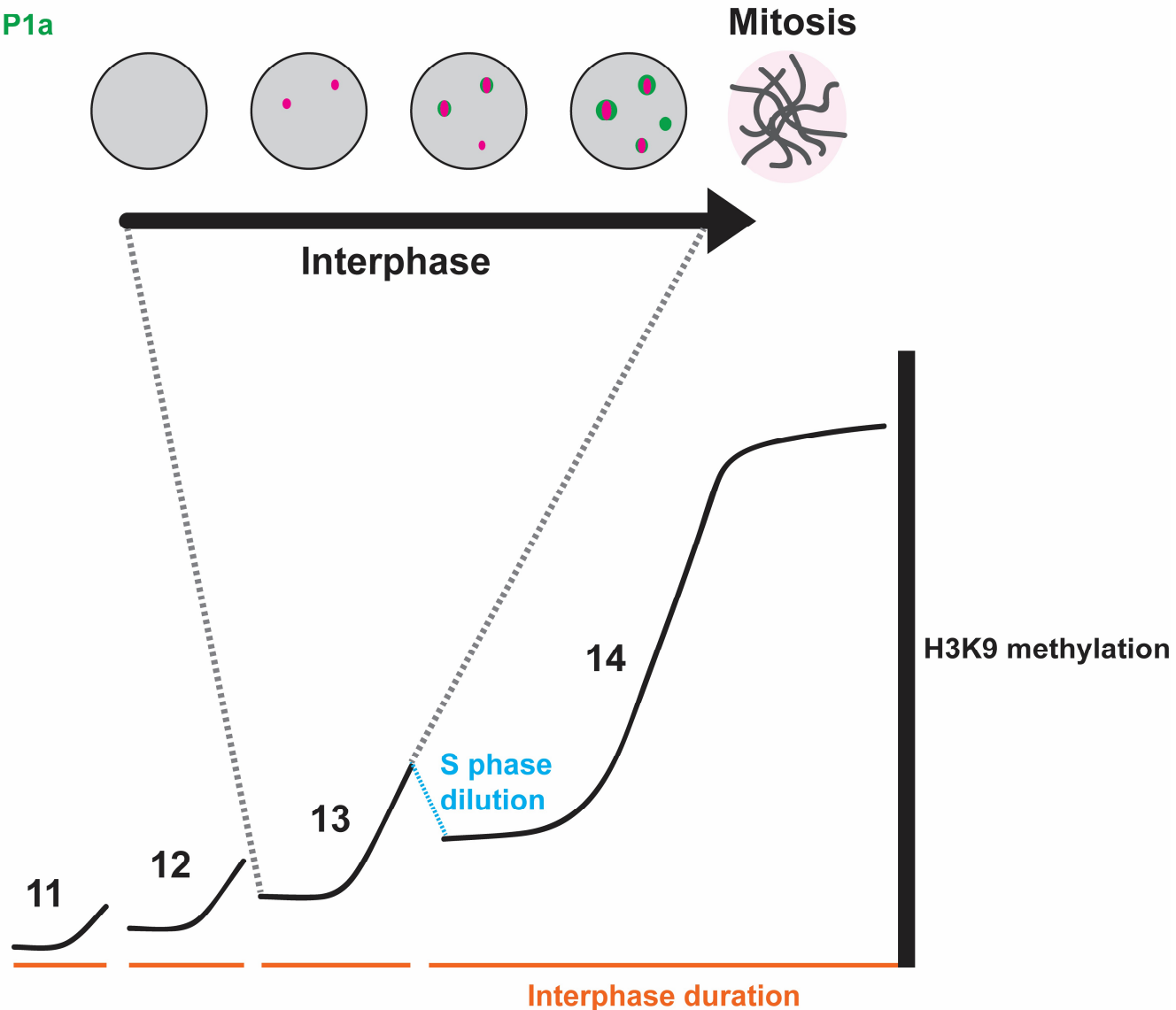
871

872

873

Eggless

HP1a



874

Figure 6. Model

875 Eggless initiates constitutive heterochromatin formation during early embryonic development. Egg is recruited
876 to chromatin foci after a delay at the start of interphase. Egg foci grow in number and intensity as interphase
877 proceeds. Later in interphase HP1a is recruited to sites occupied by Egg, although some HP1a recruitment is
878 independent of Egg. The domain of HP1a grows and extends beyond the Egg signal. Finally, chromosome
879 condensation in mitosis strips Egg from chromatin. Below a schematic showing that the progressive
880 accumulation of H3K9-methyl depends on the progressive lengthening of interphase during embryogenesis.
881 Every S phase decreases the level of modification by half due to incorporation of newly synthesized histone
882 proteins. Interphase duration limits the deposition of K9me2/3 by restricting the binding of Egg to its chromatin
883 targets, therefore high levels of modification appear only later in embryogenesis when the cell cycle slows
884 down.
885

886

887